Optimally decoding the input rate from an observation of the interspike intervals

2001 J. Phys. A: Math. Gen. 34 7475

(http://iopscience.iop.org/0305-4470/34/37/304)

INSTITUTE OF PHYSICS PUBLISHING JOURNAL OF PHYSICS A: MATHEMATICAL AND GENERAL

J. Phys. A: Math. Gen. **34** (2001) 7475–7492 PII: S0305-4470(01)22231-8

Optimally decoding the input rate from an observation of the interspike intervals

Jianfeng Feng

COGS, University of Sussex at Brighton, BN1 9QH, UK
and
Computational Neuroscience Laboratory, The Babraham Institute, Cambridge CB2 4AT, UK

E-mail: jf218@cam.ac.uk

Received 22 February 2001, in final form 30 May 2001
Published 7 September 2001
Online at stacks.iop.org/JPhysA/34/7475

Abstract

A neuron extensively receives both inhibitory and excitatory inputs. What is the ratio r between these two types of input so that the neuron can most accurately read out input information (rate)? We explore the issue in this paper provided that the neuron is an ideal observer—decoding the input information with the attainment of the Cramer–Rao inequality bound. It is found that, in general, adding certain amounts of inhibitory inputs to a neuron improves its capability of accurately decoding the input information. By calculating the Fisher information of an integrate-and-fire neuron, we determine the optimal ratio r for decoding the input information from an observation of the efferent interspike intervals. Surprisingly, the Fisher information can be zero for certain values of the ratio, seemingly implying that it is impossible to read out the encoded information at these values. By analysing the maximum likelihood estimate of the input information, it is concluded that the input information is in fact most easily estimated at the points where the Fisher information vanishes.

PACS number: 87.19.La

1. Introduction

The brain is intricately wired in such a way that a single neuron extensively receives both excitatory and inhibitory inputs. Traditionally it is believed that all information is encoded in excitatory inputs and that inhibitory inputs only play a passive role [5]. The functional role of the inhibitory input is much less well known than its counterpart, although in recent years there has been a large body of literature devoted to the issue, both theoretically and experimentally (see, for example, [12, 17, 36]).

Assume that neurons are ideal observers in the sense that they are able to *optimally* decode information: they are capable of reading out the input information with the attainment of the Cramer–Rao inequality bound (see, for example, [23], chapter 2). Suppose that $\hat{\lambda}(r)$ is an estimate of the input rate λ. We know, from the Cramer–Rao inequality that

$$\langle(\hat{\lambda}(r) - \langle\hat{\lambda}(r)\rangle)^2\rangle \geqslant \frac{(1 + (\langle\hat{\lambda}(r)\rangle - \lambda)')^2}{I(\lambda, r)}$$

where $(\ )'$ is the derivative with respect to λ and $I(\lambda, r)$ is the Fisher information about λ. Hence for any estimate $\hat{\lambda}(r)$ of λ, its accuracy (variance) is limited by the Cramer–Rao inequality bound

$$\frac{(1 + (\langle\hat{\lambda}(r)\rangle - \lambda)')^2}{I(\lambda, r)}.$$

For an unbiased estimate of the stimulus, i.e. $\langle\hat{\lambda}(r)\rangle - \lambda = 0$, according to the Cramer–Rao inequality, we know that the decoding accuracy (variance) is simply limited by the inverse of the Fisher information. Hence when the estimate of the stimulus is unbiased and attains the Cramer–Rao inequality bound which is proportional to the inverse of the Fisher information (ideal observer), we know that the larger the Fisher information is, the lower the variance of the estimate, i.e. the more accurate the estimate.

In this paper we wish to answer the following question. *What is the ratio between the inhibitory input and the excitatory input so that the neuron can optimally decode the input information*? By optimization, we mean those points of the ratio where the Fisher information attains its global maximum. Recall that the ratio r between inhibitory inputs and excitatory inputs can range from zero (purely excitatory inputs) to one (exactly balanced inhibitory and excitatory inputs) [1, 31, 33].

Using the Fisher information, we theoretically explore the issue of at which ratio r a neuron optimally reads out the input information. Although information theory has been successfully and extensively applied to neuroscience [26, 30, 35], it is generally accepted that to rigorously calculate this is still very difficult and many approximated methods have been proposed (see, for example, [21, 25] and references therein. (For the relationship between the Shannon information and the Fisher information see, for example, [23] p. 261 and also section 8.) Here we develop a method to approximate the distribution density of the efferent interspike intervals of the integrate-and-fire (IF) model, which then enables us to *rigorously* calculate the Fisher information of the IF model [16,27,34]. We find that the Fisher information reaches its global maximum when there are certain amounts of inhibitory inputs, as in realistic neuron systems where certain amounts of inhibitory inputs are always present.

When the Fisher information is positive, our results tell us that adding inhibitory inputs can improve the neuronal capability of decoding the input information and so our aforementioned question is answered. However, the other illuminating and surprising result found here is that the Fisher information can be zero at some values of the ratio $r > 0$ of the model. At these values of r where the Fisher information vanishes (we call them singular points [24]), it is theoretically impossible to estimate or decode the input information since the variance of any estimate is infinity. In statistical theory, it is conventionally assumed that the Fisher information is always greater than zero [23]. Our results in this paper provide us with a concrete example which clearly shows that the Fisher information can be zero in physiologically plausible parameter regions. The result seems counter-intuitive.

To gain a better understanding of the results above, we employ the maximum likelihood estimate to decode the input rate. When the maximum likelihood estimate exists and is unique, it is asymptotically unbiased and attains the Cramer–Rao inequality bound [23, p 444]. The

maximum likelihood estimate usually gives two solutions of the input rate in the model we consider. But when the Fisher information vanishes, there can be a unique solution. *This scenario enables us to propose a method to unambiguously read out the input information at singular points*. This conclusion differs from the traditional view that *the larger the Fisher information is, the easier it is to estimate the input information*.

Despite a century of research activity, we are still not clear how a neural system efficiently encodes and then decodes the input information [5]. One of the essential difficulties lies in the fact that neuronal responses, even to a single repeated stimulus, are typically described by stochastic models due to their inherent variability. In addition, the stimuli themselves are often described stochastically. An ideal observer, optimally decoding the input information as we discuss here, can allow us to determine limits on the accuracy and reliability of neural encoding, and possibly provide us with a 'template' of real biological neuron systems. It is obvious that reading out the input information in the neuronal system is limited by the optimal estimation. These conclusions may also be useful for the design of artificial (spiking) neuron networks, which are thought of as the new generation of neural networks. Our results tell us at which ratio r a neuron can optimally decode the input information. Furthermore, the maximum likelihood estimate provides us with a practical way to decode the input information.

The paper is organized as follows. In section 2, the IF model is introduced. In section 3, some results on the Fisher information are given and the results also give us a general idea on when and why the Fisher information can be zero. The Fisher information for the IF model is then calculated in section 4. Numerical results for calculating the Fisher information are then carried out in section 5. In section 6 the maximum likelihood estimate is developed for the model discussed in the previous two sections. Although the results discussed in sections 4–6 are based on the model with some parameter values outside physiologically reasonable regions, these results are of physical (statistical) interest. In section 7 we turn to the model with more physiologically reasonable parameters.

2. Models

For two given quantities $V_{\text{thre}} > V_{\text{rest}}$ and when $v_t < V_{\text{thre}}$, the membrane potential v_t satisfies the following dynamics:

$$\begin{aligned} \mathrm{d}v_t &= -\frac{v_t - V_{\text{rest}}}{\gamma}\,\mathrm{d}t + \mathrm{d}I_{\text{syn}}(t) \\ v_0 &= V_{\text{rest}} \end{aligned} . \tag{2.1}$$

$I_{\text{syn}}(t)$ is the synaptic input given by

$$I_{\text{syn}}(t) = \mu t + \sigma B_t \tag{2.2}$$

with constants $\mu \geqslant 0, \sigma \geqslant 0$ and the standard Brownian motion B_t. Once v_t is greater than V_{thre}, it is reset to V_{rest}. More specifically we define

$$\mu = a\lambda(1-r) \qquad \sigma^2 = a^2\lambda(1+r) \tag{2.3}$$

where a is the magnitude of EPSPs (excitatory postsynaptic potentials) and IPSPs (inhibitory postsynaptic potentials), $\lambda = \lambda_{\text{E}} N_{\text{E}}$ is the input rate with N_{E} the number of active synapses and λ_{E} the firing rate of each synapse, and r is the ratio between inhibitory inputs and excitatory inputs. Equation (2.3) implies that synaptic inputs take the form of Poisson processes [34]. In particular, when $r = 0$ the neuron exclusively receives excitatory inputs; when $r = 1$ the inhibitory and excitatory input is exactly balanced. Here, for simplicity of notation, we assume that the EPSP and IPSP size are equal. We refer the reader to [22] for a more complete and

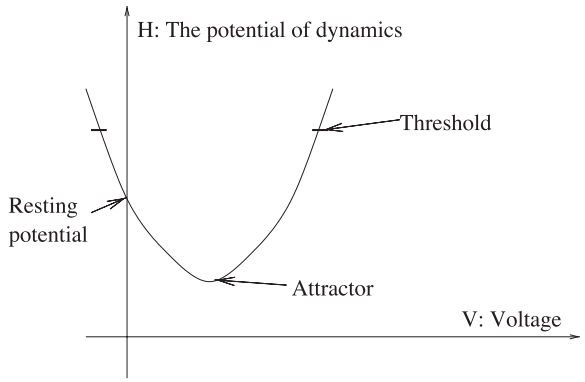

Figure 1. A schematic representation of equation (3.1). The minimum x_0 of H is the attractor of the dynamics x_t, i.e attractor $= x_0$ (see section 3 for a concrete example).

biologically oriented formulation of synaptic inputs. The model defined by equation (2.1) is called the IF model [11, 22].

In the model, there are two driving forces—the deterministic one, $\gamma\mu$, and the stochastic one, $\sigma\gamma$—that depolarize the cell to fire. When $V_{\text{thre}} < \gamma\mu$, the deterministic force alone is strong enough to ensure that the cell fires and the stochastic force is only a perturbation of the system. In this case, as we discussed in [13], the interspike intervals are usually very regular. The other case is $V_{\text{thre}} > \gamma\mu$. Now the stochastic force plays a major role to push the cell to cross the threshold. As a consequence, the cell fires with very irregular spike trains. We concentrate exclusively on the case of $V_{\text{thre}} > \gamma\mu$, i.e. the stimulus is subthreshold and efferent spike trains are irregular. As discussed in the previous section, this is the most biologically relevant case [16].

In what follows, we define

$$T(\lambda, r, \gamma) = \inf\{t : v_t \geqslant V_{\text{thre}}\} \tag{2.4}$$

as the firing time (interspike intervals) for $r \in [0, 1]$.

3. Fisher information and interspike interval distributions

Suppose that a function H has a unique minimum at x_0 and a stochastic differential equation is defined by $\mathrm{d}x_t = -H'(x_t)\,\mathrm{d}t + \sigma\,\mathrm{d}B_t$. The function H is called the potential of the dynamics x_t. Then the mean of the first hitting time T of the process x_t from $V_{\text{thre}} > x_0$ is approximately given by (see figure 1)

$$\langle T\rangle = \frac{\sqrt{\pi}\sigma}{[H'(V_{\text{thre}})]\sqrt{(H''(x_0))^{\delta}}} \exp\left(\frac{2[H(V_{\text{thre}}) - H(x_0)]}{\sigma^2}\right) \tag{3.1}$$

and furthermore

$$T \sim p(t) = \frac{1}{\langle T\rangle} \exp\left(-\frac{t}{\langle T\rangle}\right) \tag{3.2}$$

where $\delta > 0$ is a parameter. See [6] for a detailed proof of (3.1) and (3.2). Equations (3.1) and (3.2) tell us that T is exponentially distributed, i.e. the efferent spike trains of the IF model are a Poisson process with a rate $1/\langle T\rangle$. The dependence of $1/\langle T\rangle$ on the function H and model parameters V_{thre}, σ, etc is described by equation (3.1). In the next section, we apply equations (3.1) and (3.2) to the IF model.

Note that equation (3.1) (see figure 1) is different from the well known Kramer formula (see, for example, [4, 15, 28]): the pre-factor

$$\frac{\sqrt{\pi}\sigma}{[H'(V_{\text{thre}})]\sqrt{(H''(x_0))^{\delta}}}$$

on the right-hand side of equation (3.1) depends not only on H'', which is the case in Kramer's formula, but also on H'.

Suppose that $\langle T\rangle$ depends on a parameter λ. The Fisher information with respect to λ [23] is defined by

$$\begin{aligned} I(\lambda) &= \frac{1}{\langle T\rangle}\int_0^{\infty}\left(\frac{\partial \log p}{\partial\lambda}\right)^2 \exp\left(-\frac{t}{\langle T\rangle}\right)\mathrm{d}t \\ &= \frac{1}{\langle T\rangle}\int\left(\frac{(\langle T\rangle)'}{\langle T\rangle}-\frac{(\langle T\rangle)'t}{(\langle T\rangle)^2}\right)^2 \exp\left(-\frac{t}{\langle T\rangle}\right)\mathrm{d}t \\ &= \frac{[(\langle T\rangle)']^2}{[\langle T\rangle]^2} \end{aligned} \tag{3.3}$$

where $(\langle T\rangle)'$ is the derivative with respect to the parameter λ.

Equation (3.3) is the starting point for our further analysis. For Poisson process we have $\langle T\rangle = 1/\lambda$ and therefore $I(\lambda) = 1/\lambda^2 = (\langle T\rangle)^2$. The larger the $\langle T\rangle$ is, the larger the Fisher information. Instead of estimating the input firing rate, if we are interested in estimating the input interspike intervals $\langle T\rangle$, we then have $I(\langle T\rangle) = 1/(\langle T\rangle)^2$ (see table 5.1 in [23]).

In fact, from equation (3.3) it is readily seen that the Fisher information is zero whenever $(\langle T\rangle)'$ *is zero.* In other words, when $\langle T\rangle$ reaches its maximum or minimum points, the Fisher information vanishes. This also suggests that singular points are very common when we consider a nonlinear model.

4. IF model with subthreshold stimuli

As an application of the results in the previous section, we consider the IF model with subthreshold stimuli, i.e. $V_{\text{thre}} > \gamma\mu$. Let $T(\lambda, r, \gamma)$ be the interspike intervals of the IF model, defined in section 2. We can thus apply the results on T in section 3 to $T(\lambda, r, \gamma)$ and

$$I(\lambda, r, \gamma) = \frac{[(\langle T(\lambda, r, \gamma)\rangle)']^2}{[\langle T(\lambda, r, \gamma)\rangle]^2}. \tag{4.1}$$

The derivative in equation (4.1) is with respect to λ, the input information (rate). For the IF model its potential of v_t is given by (see figure 1)

$$H(x) = \frac{x^2}{2\gamma} - \mu x.$$

Therefore we have the following quantities ($x_0 = \gamma\mu$):

$$\begin{aligned} H(x_0) &= -\tfrac{1}{2}\gamma\mu^2 \\ H(V_{\text{thre}}) &= \frac{V_{\text{thre}}^2}{2\gamma} - \mu V_{\text{thre}} \\ H'(V_{\text{thre}}) &= \frac{V_{\text{thre}}}{\gamma} - \mu \\ H''(x_0) &= \frac{1}{\gamma}. \end{aligned} \tag{4.2}$$

The mean firing time is thus given by

$$\langle T(\lambda, r, \gamma)\rangle = \frac{\gamma^{1+\delta/2}\sigma\sqrt{\pi}}{V_{\text{thre}} - \gamma\mu} \exp\left(\frac{(V_{\text{thre}} - \gamma\mu)^2}{\sigma^2\gamma}\right). \tag{4.3}$$

Equation (4.3) is the reason why we use the approximation estimate, i.e. equation (3.1), rather than the rigorous one (equation (7.1)) to calculate the Fisher information. The simple form of equation (4.3) enables us to have a transparent expression of its derivative with respect to λ as follows:

$$\begin{aligned}\frac{\gamma^{1+\delta/2}\sqrt{\pi}\sigma'(V_{\text{thre}} - \gamma\mu) + \sqrt{\pi}\gamma^{2+\delta/2}\sigma\mu'}{(V_{\text{thre}} - \gamma\mu)^2} \exp\left(\frac{(V_{\text{thre}} - \gamma\mu)^2}{\sigma^2\gamma}\right)\\ + \frac{\gamma^{1+\delta/2}\sigma\sqrt{\pi}}{(V_{\text{thre}} - \gamma\mu)} \cdot \frac{-2(V_{\text{thre}} - \gamma\mu)\gamma\mu'\sigma^2\gamma - 2\sigma\sigma'\gamma(V_{\text{thre}} - \gamma\mu)^2}{(\sigma^2\gamma)^2}\\ \times \exp\left(\frac{(V_{\text{thre}} - \gamma\mu)^2}{\sigma^2\gamma}\right).\end{aligned}$$

Hence

$$\frac{(\langle T(\lambda, r, \gamma)\rangle)'}{\langle T(\lambda, r, \gamma)\rangle} = \frac{\sigma'(V_{\text{thre}} - \gamma\mu) + \sigma\gamma\mu'}{(V_{\text{thre}} - \gamma\mu)\sigma} - \frac{2(V_{\text{thre}} - \gamma\mu)\gamma\mu'\sigma^2\gamma + 2\sigma\sigma'\gamma(V_{\text{thre}} - \gamma\mu)^2}{(\sigma^2\gamma)^2}.$$

The first term in the equation above turns out to be

$$\frac{a(1+r)(V_{\text{thre}} - \gamma\mu) + 2a\lambda(1+r)\gamma a(1-r)}{2(V_{\text{thre}} - \gamma\mu)a\lambda(1+r)} = \frac{V_{\text{thre}} + \gamma\mu}{2\lambda[V_{\text{thre}} - \gamma\mu]}$$

and the second term is

$$\frac{2(V_{\text{thre}} - \gamma\mu)\gamma^2(1-r)a^3\lambda(1+r) + a^2(1+r)\gamma(V_{\text{thre}} - \gamma\mu)^2}{a^4(1+r)^2\lambda^2\gamma^2} = \frac{V_{\text{thre}}^2 - \gamma^2\mu^2}{a^2\lambda^2\gamma(1+r)}.$$

After taking some basic algebra we obtain that

$$\begin{aligned}J = \frac{(\langle T(\lambda, r, \gamma)\rangle)'}{\langle T(\lambda, r, \gamma)\rangle} &= -\frac{1}{2\lambda} - 4\gamma - \frac{V_{\text{thre}}^2}{a^2\lambda^2\gamma(1+r)}\\ &+ \frac{4\gamma}{1+r} + (1+r)\gamma + \frac{V_{\text{thre}}}{\lambda(V_{\text{thre}} - \gamma\mu)} = -J^- + J^+\end{aligned}$$

where

$$\begin{aligned}J^- &= \frac{1}{2\lambda} + 4\gamma + \frac{V_{\text{thre}}^2}{a^2\lambda^2\gamma(1+r)} > 0\\ J^+ &= \frac{4\gamma}{1+r} + (1+r)\gamma + \frac{V_{\text{thre}}}{\lambda(V_{\text{thre}} - \gamma\mu)} > 0.\end{aligned}$$

We call J^- negative Fisher information and J^+ positive Fisher information.

Note that both the positive and the negative Fisher information are decreasing functions of r. To facilitate further analysis let us define

$$V_{\text{th}} = V_{\text{thre}}/(a\lambda).$$

Then we have

$$\begin{aligned}J^- &= \frac{1}{2\lambda} + 4\gamma + \frac{V_{\text{th}}^2}{\gamma(1+r)}\\ J^+ &= \frac{4\gamma}{1+r} + (1+r)\gamma + \frac{V_{\text{th}}}{(V_{\text{th}} - \gamma(1-r))}.\end{aligned}$$

At $r = 0$ we obtain

$$J^- = \frac{1}{2\lambda} + 4\gamma + \frac{V_{\rm th}^2}{\gamma} \qquad J^+ = 5\gamma + \frac{V_{\rm th}}{(V_{\rm th} - \gamma)}$$

and

$$J^+ - J^- = \gamma + \frac{V_{\rm th}}{V_{\rm th} - \gamma} - \frac{1}{2\lambda} - \frac{V_{\rm th}^2}{\gamma}. \tag{4.4}$$

Analogously, at $r = 1$ we arrive at

$$J^+ - J^- = \frac{1}{2\lambda} - \frac{V_{\rm th}^2}{2\gamma}.$$

Since we are considering the case that $V_{\rm thre}^2 > aV_{\rm thre} > a^2\gamma\lambda$ with $\gamma\lambda > 1$ (see section 5), we have

$$J^+ - J^- < 0$$

at $r = 1$.

The analysis above allows us to concentrate on the behaviour of $J^+ - J^-$ at $r = 0$. We have the following two cases.

- $J^+ - J^- \geqslant 0, r = 0$. Hence there is a $r_0, 0 \leqslant r_0 < 1$, at which $J^+ - J^- = 0$. The ideal observer will try to avoid the point $r = r_0$ at which $I(\lambda, r_0, \gamma) = \infty$. According to the property of the Fisher information and the conventional theory in statistics, we know that at $r = r_0$, any estimate is unreliable in the sense that its variance is infinity (however, see section 6). From equation (4.4) we know that this happens when $\gamma \sim V_{\rm th}$ or, in other words, when the deterministic part of the input closes to its threshold (see next section).
- $J^+ - J^- < 0, r = 0$. This happens when $\gamma \ll V_{\rm th}$. In this case the neuron fires slowly since the input is very weak. It is illuminating to see that there is a global minimum for the Fisher information for $r \in [0, 1]$ (see next section).

Now we present numerical results for the two cases discussed above.

5. Numerical results

We use the following set of parameters in simulations: $\gamma \in [0.15, 0.22]$ ms, $\lambda = 400 \times 0.1$ kHz, $v_{\rm thre} = 15$ mV, $\delta = 0.8$, $a = 1.4$ mV and $v_{\rm rest} = 0$ mV. The choice of γ here is for the purpose of the application of results in the previous section and is of physical interest. See section 7 for results on γ within physiologically reasonable regions. For the choice of other parameters, see [8, 9, 11, 13, 14, 16] and references therein.

For all calculations below, we use a step size of 0.01 to solve equation (2.1) and $N = 10\,000$ interspike intervals, denoted as T_i, $i = 1, \ldots, N$, are generated for estimating mean, variance, etc.

Figure 2 shows a comparison between equation (4.3) and numerical simulations for $\gamma = 0.15, 0.20, 0.22$. It is clearly seen that equation (4.3) gives a reasonably good approximation for all the parameters we considered. Furthermore, the mean of interspike intervals equals its standard deviation, inside the parameter regions we consider, which implies that the spike trains of the IF model are approximately Poisson processes. The reason we confine ourselves to $\gamma \in [0.15, 0.22]$ is that when $\gamma > 0.26$ the requirement of $V_{\rm thre} > \gamma a\lambda$ is violated; when $\gamma < 0.10$ the model neuron fires so slowly that it is completely outside the physiologically interesting region of neuron firing rates.

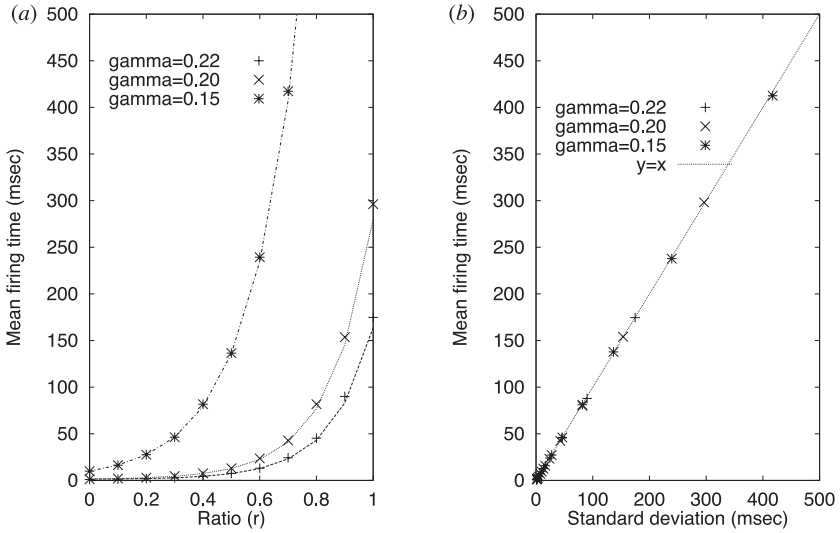

Figure 2. Mean firing time versus ratio (a) for $\gamma = 0.15, 0.20, 0.22$. Points are numerical simulations and curves are obtained in terms of equation (4.3). Meaning firing time versus standard deviation (b) for $\gamma = 0.15, 0.20, 0.22$. We see that meaning firing time $\sim$ standard deviation.

Figure 3 depicts the Fisher information versus ratio r for $\gamma = 0.20$. We can see that there is a global maximum for the Fisher information. Increasing or decreasing the inhibitory input will result in a reduction of the Fisher information. In other words, for the given parameters of the model, when r is around 0.6, the input information can be most accurately read out.

Figure 4 shows more plots of the Fisher information versus r. A comparison of figures 3 and 4 tells us that when γ decreases, the peak of the Fisher information moves to the left (small r).

When $\gamma = 0.22, 0.23$, as indicated in our theoretical results in the previous section, there is a point r_0, depending on γ, at which the Fisher information is zero. We call the point a *singular* point since at the point the variance of any estimate is infinity. At first glance, it is very puzzling to have such a singular point r_0. To the best of our knowledge, all existing statistical theories avoid discussing singular points [23, 24]. What is the actual implication of the singular point for practical estimation of the input frequency? We explore this issue in the next section.

Although the Fisher information has been extensively applied to neuroscience, as we mentioned earlier, it seems that the novel phenomena reported here have not been noted in the literature.

6. Maximum likelihood estimate

In this section we use the maximum likelihood estimate approach to estimate the input frequency λ. The approach also helps us to understand the curious phenomenon that the Fisher information calculated in the previous section attains zero and to develop a method to estimate input rate at the singular points.

After some basic calculations we see that the maximum likelihood estimate of λ is the

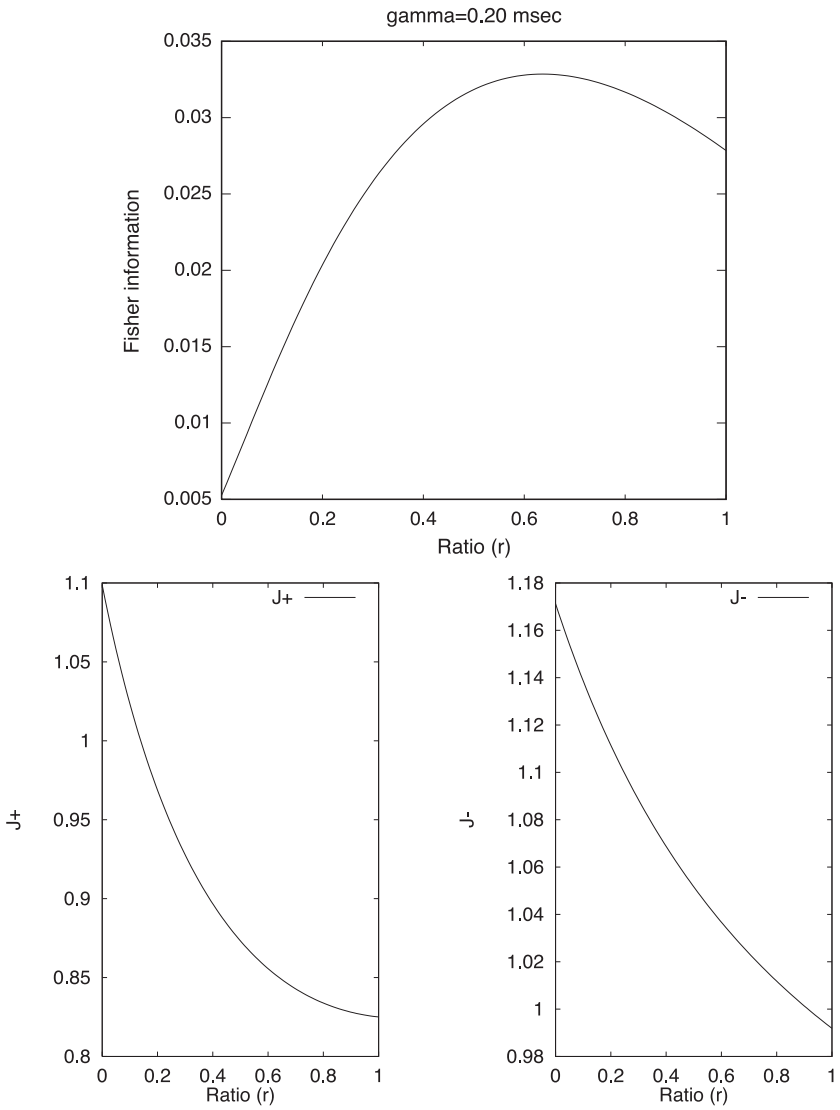

Figure 3. The Fisher information and J^+, J^- versus ratio r for $\gamma = 0.20$. It is readily seen that when r is around 0.6, the Fisher information reaches its global maximum. Both J^+, J^- are decreasing functions of r.

intersection of the function

$$f(\lambda) = \frac{(V_{\text{thre}} - \gamma\mu)^2}{\sigma^2\gamma} - \log(V_{\text{thre}} - \gamma\mu) + \log[\gamma^{1+\delta/2}\sigma\sqrt{\pi}] \tag{6.1}$$

with $\log((\sum_i T_i)/N)$, where T_i is the first hitting time (interspike intervals) obtained from numerical simulations. Note that $f(\lambda)$ is only defined for $V_{\text{thre}} > \gamma\mu$. The maximum likelihood estimator of λ is given by

$$\hat{\lambda} \in \begin{cases} A = f^{-1}\left(\log\left(\sum_i T_i/N\right)\right) & \text{if} \quad A \neq \Phi \\ \{+\infty\} & \text{otherwise.} \end{cases} \tag{6.2}$$

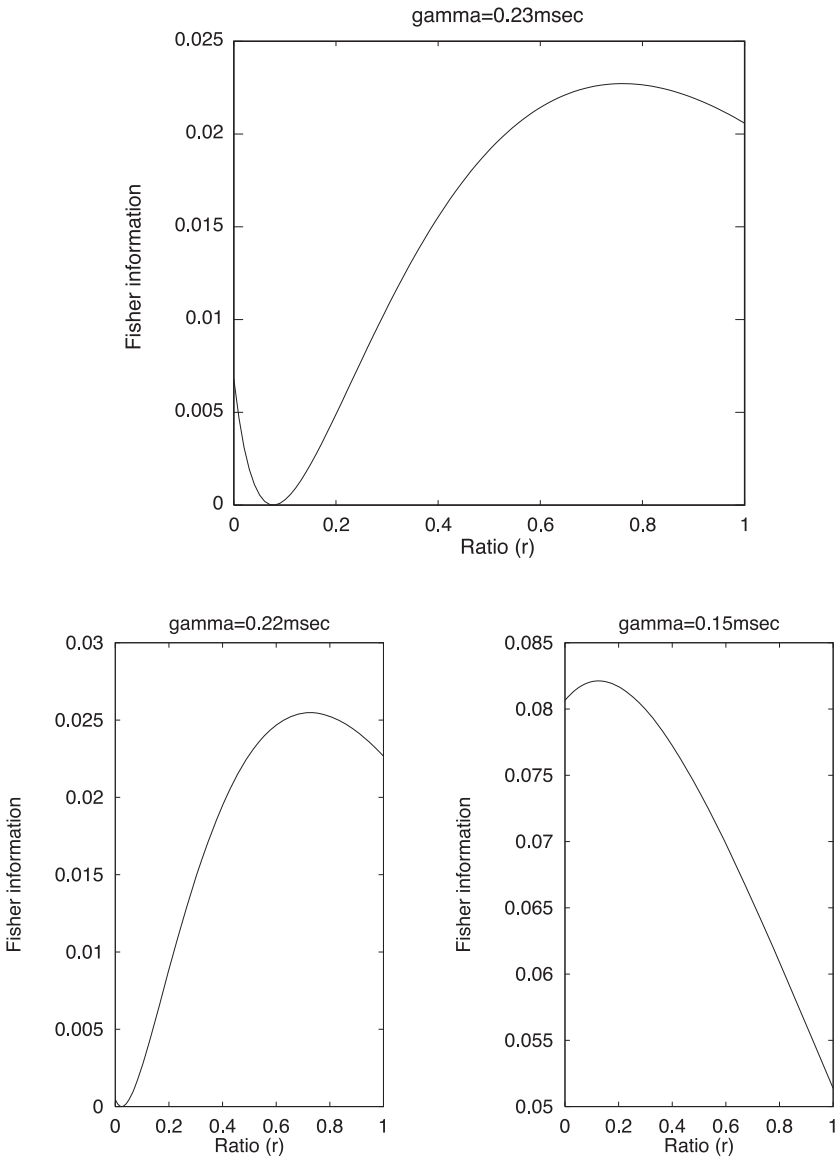

Figure 4. The Fisher information versus ratio r for $\gamma = 0.23, 0.22, 0.15$ ms. For all cases there are global maxima for the Fisher information. It is very interesting to note that when $\gamma = 0.22, 0.23$, there is a r_0, depending on γ and close to $r = 0$, at which the Fisher information is zero.

Since in general we would expect that f is not a monotonic function of λ, for a given constant a, $f^{-1}(a)$ is defined as the set of λ satisfying $f(\lambda) = a$. From equation (3.3) we see that the Fisher information vanishes if and only if $f(\lambda)$ attains its local minima or maxima, provided that $\langle T(\lambda, r, \gamma)\rangle < \infty$.

Equation (6.2) now gives us a very clear picture of the behaviour of the maximum likelihood estimate at the points where the Fisher information vanishes. Suppose that $f(\lambda)$ takes the form as in figure 5 and therefore at $\lambda = \lambda_0$ the Fisher information is zero. According

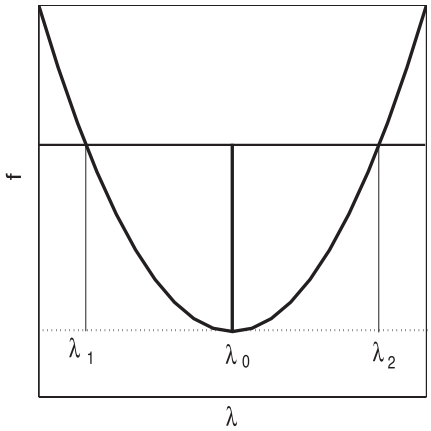

Figure 5. A schematic representation of the maximum likelihood estimate. When $\lambda \neq \lambda_0$, the maximum likelihood estimate will give us two solutions (λ_1, λ_2), indicated by thin vertical lines. When $\lambda = \lambda_0$ (indicated by thick vertical lines), by equation (6.4), the unique estimate of λ_0 is obtained, although now the Fisher information is zero and the mean of $\hat{\lambda}$ is infinity.

to equation (6.2) we have

$$\hat{\lambda} \in \begin{cases} A = f^{-1}\left(\log\left(\sum_i T_i/N\right)\right) & \text{if} \quad \log\left(\sum_i T_i/N\right) \geqslant f(\lambda_0) \\ \{+\infty\} & \text{if} \quad \log\left(\sum_i T_i/N\right) < f(\lambda_0). \end{cases} \tag{6.3}$$

When $\lambda = \lambda_0$, we see that due to the fluctuation of $\sum_i T_i/N$, $\hat{\lambda}$ will be finite, i.e. in set A, with a positive probability and be infinity with a positive probability as well. Hence the expectation of $\hat{\lambda}$ is infinity already. For the general case of f with multi-local minima or maxima, the conclusions above are also true.

Suppose that we only have a unique minimum point of $f(\lambda)$ which is true for all cases considered in this paper. In other words, the singular point of the Fisher information is unique (the following idea could be easily generalized to multi-minima (maxima) cases). At the singular point, an efficient way to estimate the input frequency is then

$$\hat{\lambda} = \lambda_0 = \begin{cases} f^{-1}\left(\log\left(\sum_i T_i/N\right) - \epsilon_1\right) & \text{if} \quad \log\left(\sum_i T_i/N\right) \geqslant f(\lambda_0) \\ f^{-1}\left(\log\left(\sum_i T_i/N\right) + \epsilon_2\right) & \text{if} \quad \log\left(\sum_i T_i/N\right) < f(\lambda_0) \end{cases} \tag{6.4}$$

where $\epsilon_1 = \log(\sum_i T_i/N) - f(\lambda_0)$ and $\epsilon_2 = -\log(\sum_i T_i/N) + f(\lambda_0)$. Note that, different from equations (6.2) and (6.3), in (6.4) the equality holds true. In practical applications, we could use small perturbations to find ϵ_1 and ϵ_2 (we shall report this in a statistical journal).

Therefore, at the singular point the maximum likelihood estimate gives us a unique solution (equation (6.4)) and at all other points the maximum likelihood estimate gives two solutions (see figure 5). Usually, it is difficult to choose one of the two solutions (see below). In this sense the input rate can be most easily and accurately read out when the Fisher information is zero.

We now turn to our neuronal models. We use all parameters as in the previous section and therefore the true value of the input frequency is 40 kHz.

In figure 7 ($\gamma = 0.22$) we plot $f(\lambda)$ against λ and therefore the intersections of $f(\lambda)$ with $\log((\sum_i T_i)/N)$ give us maximum likelihood estimates. For example, when $r = 0.04$ we have the unique solution which is the true value. Note that in figure 4, the Fisher information is zero when $r = 0.04$. Hence in terms of the maximum likelihood estimate, the singular point means that there is a unique solution for the maximum likelihood estimate. *We naturally*

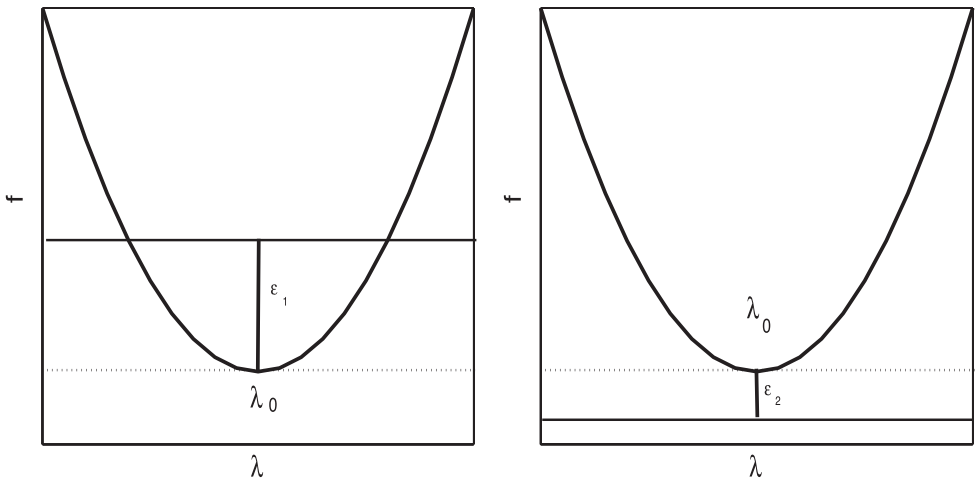

Figure 6. A schematic explanation of equation (6.4). The thick horizontal line is $\log(\sum_i T_i)/N$. When N is large, $\log(\sum_i T_i)/N$ is within an $\epsilon > \max(\epsilon_1, \epsilon_2)$ distance from $f(\lambda_0)$. If $\log(\sum_i T_i)/N > f(\lambda_0)$ (left), the maximum likelihood estimate gives us two solutions. However, we can move $\log(\sum_i T_i)/N$ downward by a distance of ϵ_1 and the maximum likelihood yields the unique, true solution λ_0. If $\log(\sum_i T_i)/N < f(\lambda_0)$ (right), the maximum likelihood estimate gives us no solution. However, we can move $\log(\sum_i T_i)/N$ upward by a distance of ϵ_2 and the maximum likelihood yields the unique, true solution λ_0.

envisage that at a singular point, we can most easily and accurately estimate the input rate, as discussed before. The traditional view that the larger the Fisher information is, the more accurately or easily we can estimate the parameter holds true for the parameter regions in which the Fisher information does not vanish. If the Fisher information reaches zero, then the conclusion is totally different, at least for the model we consider in this paper. Suppose that there is only one point in the whole parameter space at which the Fisher information vanishes, then we can estimate the parameter at the singular point most easily and accurately, in terms of the maximum likelihood estimate (see equation (6.4)). When $r > 0.04$, there are always two solutions, although one of them might be closer to the true value.

It is illuminating to compare figure 8 ($\gamma = 0.20$) with figure 7. For $\gamma = 0.20$ from figure 3 we see that the Fisher information is positive for all $r \in [0, 1]$ and hence there is no singular point. Figure 8 clearly shows that although there are two solutions, sometimes we can easily discard one which is further away from the true value and outside the physiologically reasonable parameter regions. For example, in both figures 7 and 8, when $r = 1$, we can confine ourselves to inputs smaller than 200 kHz and there is a unique solution of the maximum likelihood estimate. However, when both solutions are inside physiologically reasonable regions, it is difficult to choose between the two solutions: see, for example, when $r = 0.04$ in figure 8.

7. More realistic inputs

In the previous sections, we have considered the case that the inhibitory input is fixed, i.e. it is independent of the excitatory input. However, in general it is believed that the strength of the inhibitory input exhibits a 'push–pull' effect [7]: the stronger the excitatory input is, the stronger the inhibitory input. For simplicity of notation, as in [3] (figure 4), we assume that in equation (2.3) $r = \lambda_E N_E/(\lambda_{max} N_E)$ where λ_{max} is the maximum excitatory input rate of each

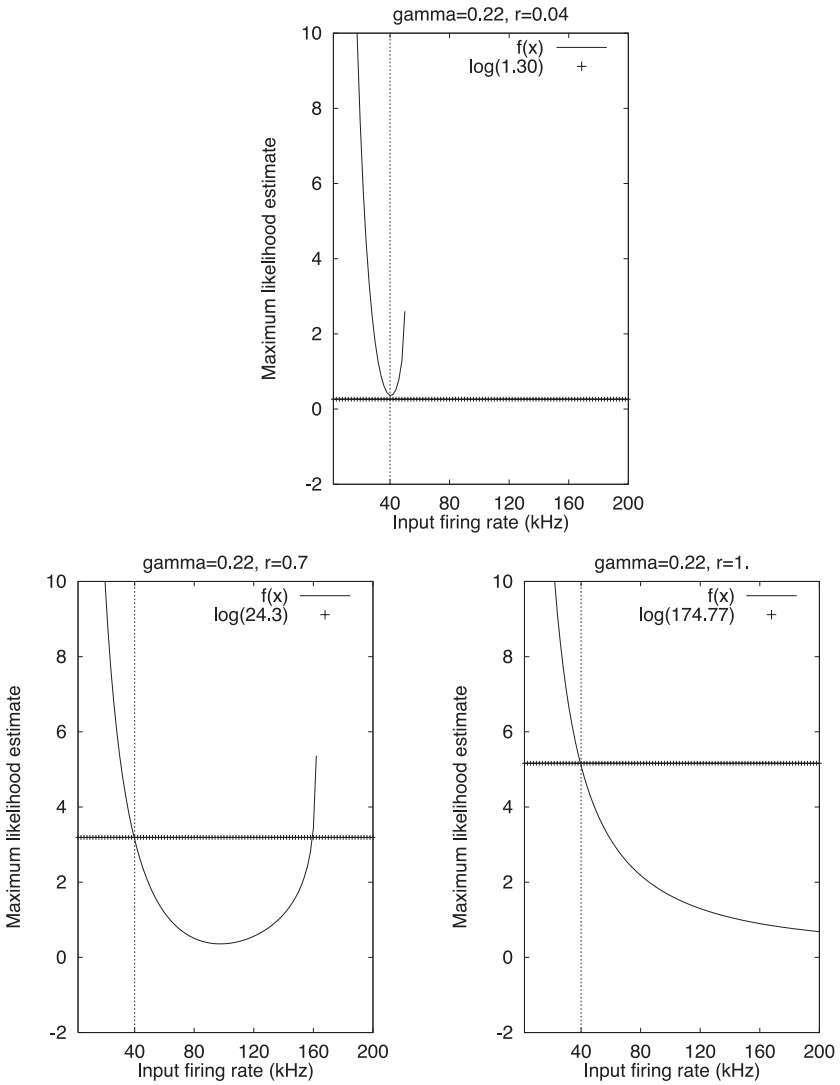

Figure 7. $F(\lambda)$ versus λ. The intersection of $f(\lambda)$ with $\log((\sum_i T_i)/N)$ gives the maximum likelihood estimate, where $N = 10\,000$ and T_i is the interspike interval. Compare with figure 4.

synapse.

We use the following rigorous results to calculate the mean firing time [19]:

$$\begin{aligned}\langle T(\lambda, r, \gamma)\rangle &= 2\int_{V_{\text{rest}}}^{V_{\text{thre}}} \frac{1}{a^2\lambda(1+r)} \exp\left(\frac{\gamma^{-1}x^2 - 2a\lambda x(1-r)}{a^2\lambda(1+r)}\right) \\ &\quad \times\left(\int_{-\infty}^{x} \exp\left(-\frac{\gamma^{-1}u^2 - 2a\lambda u(1-r)}{a^2\lambda(1+r)}\right)\mathrm{d}u\right)\mathrm{d}x \\ &= \frac{2}{a^2\lambda(1+r)}\int_{V_{\text{rest}}}^{V_{\text{thre}}} \exp\left(\frac{\gamma^{-1}(x - a\lambda(1-r)/\gamma^{-1})^2}{a^2\lambda(1+r)}\right)\exp\left(-\frac{(a\lambda(1-r))^2}{a^2\gamma^{-1}\lambda(1+r)}\right)\end{aligned}$$

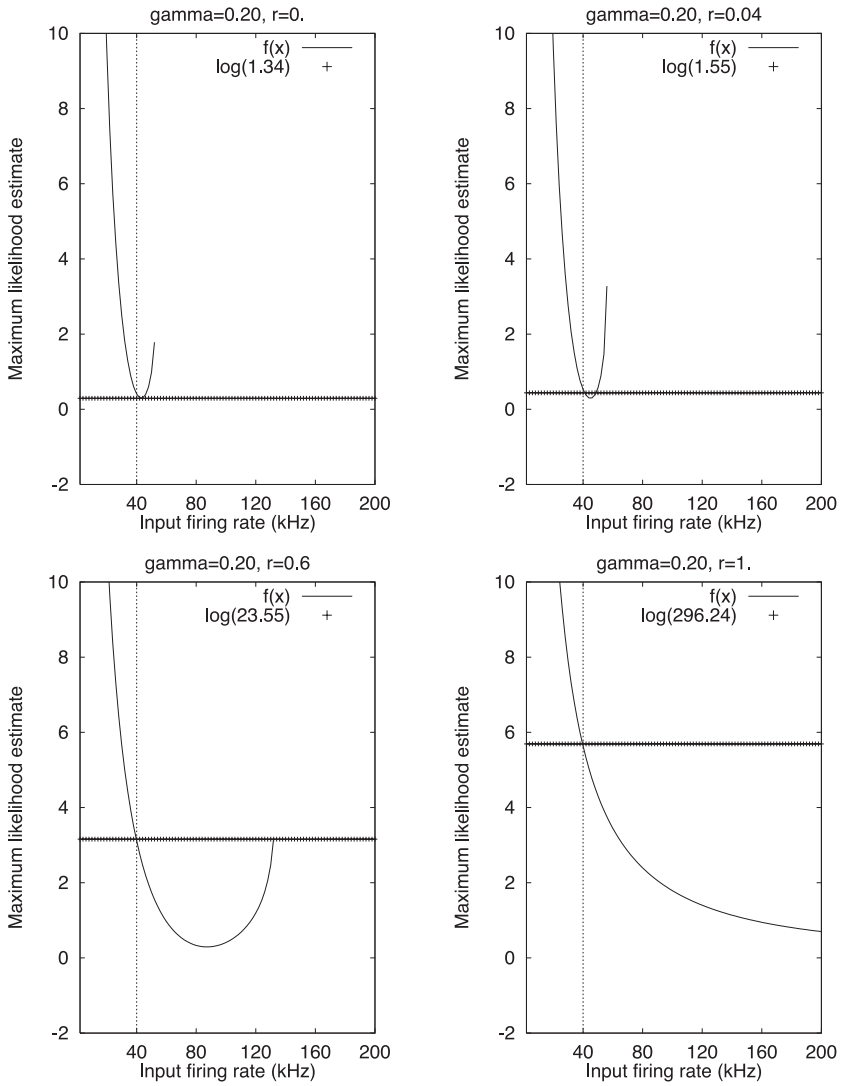

Figure 8. $F(\lambda)$ versus λ. The intersection of $f(\lambda)$ with $\log((\sum_i T_i)/N)$ gives the maximum likelihood estimate, where $N = 10\,000$ and T_i is the interspike interval. Compare with figures 4 and 7.

$$\times\left[\int_{-\infty}^{x}\exp\left(-\frac{\gamma^{-1}(u-a\lambda/\gamma^{-1})^2}{a^2\lambda(1+r)}\right)\mathrm{d}u\right]\exp\left(\frac{(a\lambda(1-r))^2}{a^2\gamma^{-1}\lambda(1+r)}\right)\mathrm{d}x$$
$$=\frac{2}{a^2\lambda(1+r)}\int_{V_{\rm rest}}^{V_{\rm thre}}\exp\left(\frac{\gamma^{-1}(x-a\lambda(1-r)/\gamma^{-1})^2}{a^2\lambda(1+r)}\right)$$
$$\times\left[\int_{-\infty}^{x}\exp\left(-\frac{\gamma^{-1}(u-a\lambda/\gamma^{-1})^2}{a^2\lambda(1+r)}\right)\mathrm{d}u\right]\mathrm{d}x$$
$$=\frac{2}{\gamma^{-1}}\int_{\frac{V_{\rm rest}\sqrt{\gamma^{-1}}}{a\sqrt{\lambda(1+r)}}-\frac{\sqrt{\lambda}(1-r)}{\sqrt{\gamma^{-1}(1+r)}}}^{\frac{V_{\rm thre}\sqrt{\gamma^{-1}}}{a\sqrt{\lambda(1+r)}}-\frac{\sqrt{\lambda}(1-r)}{\sqrt{\gamma^{-1}(1+r)}}}\left[\exp(x^2)\int_{-\infty}^{x}\exp(-u^2)\,\mathrm{d}u\right]\mathrm{d}x. \tag{7.1}$$

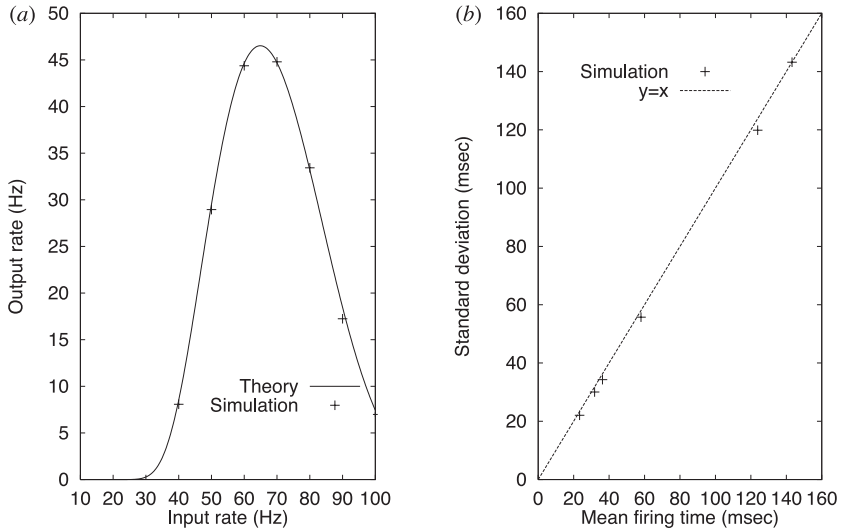

Figure 9. (*a*) Output firing rate versus input firing rate (λ_E). Points are obtained in terms of numerical simulations. (*b*) The mean firing time against standard deviation. Parameters are $\gamma = 1$ ms, $a = b = 1$ mV, $V_{thre} = 20$ mV, $V_{rest} = 0$ mV, $N_E = 400$, $\lambda_{max} = 100$ Hz. Parameters are chosen so that all stimuli are subthreshold and input, output firing rates are in physiologically plausible regions, between 0 and 100 Hz.

In figure 9(*a*) we plot the output firing rate versus input firing rate of the IF model with its inhibitory input rate proportional to its excitatory input rate. Note that when $\lambda_E = \lambda_{max}/2$, the mean input μ attains its global maximum. In our case, it is 50 Hz. However, there is a shift to the right for the output firing rate to attain its maximum, i.e. it reaches its maximum firing rate at $\lambda_E = 65$ Hz, $r = 0.65$. This is simply due to the fact that both the mean and variance of inputs contribute to push the neuron to fire. Figure 9(*b*) depicts the mean firing time against standard deviation, which indicates that the efferent spike train is approximately a Poisson process.

The drawback of the monotonic input–output relationship of a neuron, namely the well known sigmoidal function, has been criticized in [3] and elsewhere. In fact, from the dynamical system point of view, a monotonic input–output relationship implies that there are only two stable attractors. Therefore, after transformation of a few layers, neuronal activities either become totally silent or fire at a fixed rate—seeing either 'black' or 'white', but not 'colour'. A non-monotonic relationship of input–output as in figure 9 considerably enriches neuronal activities. Depending on its parameters, it can exhibit chaotic behaviour. Other biophysical mechanisms to generate the non-monotonic input–output relationship include synaptic depression [2], and low-threshold calcium current [37], etc.

According to the theory developed in the previous sections, we assert that for the input–output relationship depicted in figure 9, when the input rate is at 65 Hz, the Fisher information is zero and so we can most easily read out the input rate. More specifically, the Fisher information is now

$$I(\lambda, r, \gamma) = \frac{[(\langle T(\lambda, r, \gamma)\rangle)']^2}{[\langle T(\lambda, r, \gamma)\rangle]^2} \tag{7.2}$$

and the maximum likelihood estimate is given by the solution of

$$\langle T(\lambda, r, \gamma)\rangle = \sum T_i/N.$$

Note that when the input is 65 Hz the neuron fires at its maximal firing rate. It is generally accepted that the faster the neuron fires, the more information it carries. In other words, $\lambda_E = 65$ Hz is the most important point for the neuron to read out.

It is also very interesting to note that neuronal response curves [18] exhibit a similar (bell) shape of input–output relationship as in figure 9. Therefore our results developed here can also be applied to population coding theory.

8. Discussion

With a fixed excitatory input to a neuron, we ask how strong the inhibitory input to the neuron is required to be for optimal decoding of the input information based upon an observation of the efferent spike trains. We find that usually certain amounts of inhibitory inputs are needed to ensure that the Fisher information attains its global maximum. Although it is well known that the inhibitory input is present in real neuron systems and a number of functional roles for it have been put forward in recent years [10, 36], it seems that we are the first to address the issue in terms of the Fisher information. The conclusions obtained here should also be useful for the design of spiking neural networks for engineering applications.

A somewhat surprising result is that the Fisher information is zero at some points of the ratio. Using the maximum likelihood estimate, we find that at singular points there is a unique solution. We then articulate that at the singular point, we can most easily estimate the input rate. In summary let us define

$$\mathcal{R}_0 = \{r : I(\lambda, r, \gamma) = 0, r \neq 0, 1\}$$
$$\mathcal{R}_m = \{r : I(\lambda, r, \gamma) \text{ attains its local maximum }, r \neq 0, 1\}.$$

Inhibitory inputs ensure that $\mathcal{R}_0 \cup \mathcal{R}_m$ is not an empty set. Parameters inside $\mathcal{R}_0$ are more easily estimated than those inside $\mathcal{R}_m$.

Within a totally different context, a related issue has been addressed in the literature in the past few years. It is articulated in [29] that if only excitatory inputs are presented, a model neuron with integrate and fire mechanisms fires very regularly and therefore its behaviour contradicts cortical neuron behaviour. Shadlen and Newsome [31] then showed that if an exactly balanced inhibitory input and excitatory input is presented, the efferent spike trains of a single neuron model are very irregular. It would seem that a neuron operates in an environment of exactly balanced inputs. However, we [8, 9, 13, 14, 16] have shown that the picture is much more complex than the aforementioned results. A neuron can easily generate irregular firing patterns, no matter whether it receives a purely excitatory input or an exactly balanced input. Hence the question of which regions of the ratio a neuron operates in remains elusive. An answer would be informative and shed new light on the fundamental issue in neuroscience: How do neural systems organize, at least locally, to process information? The results presented in this paper provide some clues.

The IF model is the simplest model in theoretical neuroscience, which reflects certain aspects of a real neuron and provides us with some clues on how a real neuron operates [2, 11]. It would be interesting to apply our conclusions to more biologically realistic models, to the framework of population coding theory [18,20] and to models with correlated inputs [16,32,38].

The most common quantity about information used in neuroscience is the Shannon information. We cite the relationship between the Shannon information and the Fisher information here [23].

Theorem 1. *Let $T_1, \ldots, T_N$ be an iid sample from $f(t|\lambda)$ with the priori $\pi(\lambda)$, and let $S_N(\pi)$*

denote the Shannon information of the sample. Then as $N \to \infty$

$$S_N(\pi) = \frac{k}{2} \log \frac{N}{2\pi e} + \int \pi(\lambda) \log \frac{|I(\lambda)|^{1/2}}{\pi(\lambda)} \, d\lambda + o(1) \tag{8.1}$$

where k *is the dimension of* λ.

Equation (8.1) gives us a transparent and interesting relationship between the Shannon information which has been intensively applied to neuroscience in recent years and the Fisher information which we have explored here. However, it seems that no one has investigated them according to equation (8.1), which might shed new light on some of the issues discussed here.

Acknowledgments

This work has been partially supported by BBSRC and an ESEP grant of the Royal Society.

References

[1] Abeles M 1990 *Corticonics* (Cambridge: Cambridge University Press)
[2] Abbott L F, Varela J A, Sen K and Nelson S B 1997 Synaptic depression and cortical gain control *Science* **275** 220–3
[3] Abbott L F 1991 Realistic synaptic inputs for model neural networks *Network: Comput. Neural Syst.* **2** 245–58
[4] Albeverio S, Feng J and Qian M 1995 Role of noise in neural networks *Phys. Rev.* E **52** 6593–606
[5] Albright T D, Jessell T M, Kandel E R and Posner M I 2000 Neural science: a century of progress and the mysteries that remain *Cell* **100** s1–55
[6] Aldous D 1989 *Probability Approximation Via the Poisson Clumping Heuristic* (Berlin: Springer)
[7] Benyishai R, Baror R L and Sompolinsky H 1995 Theory of orientation tuning in visual-cortex *Proc. Natl Acad. Sci. USA* **92** 3844–8
[8] Brown D and Feng J 1999 Is there a problem matching model and real CV(ISI)? *Neurocomputing* **26–7** 117–22
[9] Brown D, Feng J and Feerick S 1999 Variability of firing of Hodgkin–Huxley and FitzHugh–Nagumo neurons with stochastic synaptic input *Phys. Rev. Lett.* **82** 4731–4
[10] Feerick S, Feng J and Brown D 2000 Increasing inhibition can boost a neuron's firing rate, submitted
[11] Feng J 1997 Behaviours of spike output jitter in the integrate-and-fire model *Phys. Rev. Lett.* **79** 4505–8
[12] Feng J 2001 Is the integrate-and-fire model good enough?—a review *Neural Netw.* at press
[13] Feng J and Brown D 1998 Impact of temporal variation and the balance between excitation and inhibition on the output of the perfect integrate-and-fire model *Biol. Cybern.* **78** 369–76
[14] Feng J and Brown D 1999 Coefficient or variation greater than 0.5 how and when? *Biol. Cybern.* **80** 291–7
[15] Feng J and Brown D 2000 Integrate-and-fire models with nonlinear leakage *Bull. Math. Biol.* **62** 467–81
[16] Feng J and Brown D 2000 Impact of correlated inputs on the output of the integrate-and-fire model *Neural Comput.* **12** 671–92
[17] Feng J, Brown D and Li G 2000 Synchronization due to common pulsed input in Stein's model *Phys. Rev.* E **61** 2987–95
[18] Feng J and Cassia-Moura R 1999 Output of a neuronal population code *Phys. Rev.* E **59** 7246–9
[19] Feng J and Wei G 2001 Increasing inhibitory input *increases* neuronal firing rate: why and when? *J. Phys. A: Math. Gen.* **34** 7493–509 (following paper)
[20] Gerstner W, Kreiter A K, Markram H and Herz A V M 1997 Neural codes: firing rates and beyond *Proc. Natl Acad. Sci. USA* **94** 12740–1
[21] Golomb D, Hertz J, Panzeri S, Treves A and Richmond B 1997 How well can we estimate the information carried in neuronal responses from limited samples? *Neural Comput.* **9** 649–65
[22] Koch C 1999 *Biophysics of Comput.* (Oxford: Oxford University Press)
[23] Lehmann E and Casella G 1999 *Theory of Point Estimation* (Berlin: Springer)
[24] Liu R C and Brown L d 1993 Nonexistence of informative unbiased estimators in singular problems *Ann. Stat.* **21** 1–13
[25] Pincus S and Singer B H 1998 A recipe for randomness *Proc. Natl Acad. Sci. USA* **95** 10367–72
[26] Rieke F, Warland D, van Steveninch R R D and Bialek W 1997 *Spikes: Exploring the Neural Code* (Cambridge, MA: MIT Press)

[27] Ricciardi L M and Sato S 1990 Diffusion process and first-passage-times problems *Lectures in Applied Mathematics and Informatics* ed L M Ricciardi (Manchester: Manchester University Press)
[28] Risken S 1989 *The Fokker–Planck Equation* (Berlin: Springer)
[29] Softky W and Koch C 1993 The highly irregular firing of cortical-cells is inconsistent with temporal integration of random EPSPs *J. Neurosci.* **13** 334–50
[30] Strong S P, Koberle R, van Steveninck R R D and Bialek W 1998 Entropy and information in neural spike trains *Phys. Rev. Lett.* **80** 197–200
[31] Shadlen M N and Newsome W T 1994 Noise, neural codes and cortical organization *Curr. Opin. Neurobiol.* **4** 569–79
[32] Stevens C F and Zador A M 1998 Input synchrony and the irregular firing of cortical neurons *Nat. Neurosci.* **1** 210–7
[33] Tsodyks M V, Skaggs W E, Sejnowski T J and McNaughton B L 1997 Paradoxical effects of external modulation of inhibitory interneurons *J. Neurosci.* **17** 4382–8
[34] Tuckwell H C 1988 *Introduction to Theoretical Neurobiology* vol 2 (Cambridge: Cambridge University Press)
[35] van Steveninck R R D and Laughlin S B 1996 The rate of information transfer at graded-potential synapses *Nature* **379** 642–5
[36] van Vereeswijk C, Abbott L F and Ermentrout G B 1994 When inhibition not excitation synchronizes neural firing *J. Comput. Neurosci.* **1** 313–21
[37] Williams S R, Toth T I, Turner J P, Hughes S W and Crunelli V 1997 The 'window' component of the low threshold $Ca2^{+}$ current produces input signal amplification and bistability in cat and rat thalamocortical neurones *J. Physiol. (Lond.)* **505** 689–705
[38] Zohary E, Shadlen M N and Newsome W T 1994 Correlated neuronal discharge rate and its implications for psychophysical performance *Nature* **370** 140–3